Journal of the American College of Cardiology
© 2007 by the American College of Cardiology Foundation
Published by Elsevier Inc.

Vol. 49, No. 12, 2007
ISSN 0735-1097/07/$32.00
doi:10.1016/j.jacc.2006.10.075

PRECLINICAL STUDIES

Unique Autonomic Profile of the Pulmonary Veins and Posterior Left Atrium

Rishi Arora, MD, Jason Ng, PhD, Joseph Ulphani, MD, Ilias Mylonas, MD, Haris Subacius, PhD, Greg Shade, BS, David Gordon, MD, PhD, Alexander Morris, BS, Xiang He, MS, Yi Lu, MD, Rashad Belin, PhD, Jeffrey J. Goldberger, MD, Alan H. Kadish, MD

Chicago, Illinois

Objectives The purpose of this study was to investigate the electrophysiologic profile of the pulmonary veins (PVs) and left atrium (LA) in response to autonomic manipulation.

Background The parasympathetic innervation of the PVs and posterior left atrium (PLA) is thought to contribute to focal atrial fibrillation (AF). We hypothesized that autonomic effects would be more prominent in these regions.

Methods In 14 dogs, epicardial mapping was performed in the PVs, PLA, and left atrial appendage (LAA) under the following conditions: baseline, 20-Hz cervical vagal stimulation (VS), propranolol (P), P + VS, and P + atropine. Effective refractory periods (ERPs) were measured, and conduction vectors were computed at multiple sites. Western blotting and immunostaining were performed for IKAch (Kir3.1/3.4).

Results The VS and P + VS caused more ERP shortening in the PV and PLA than in the LAA. The P + atropine caused greatest ERP prolongation in the LAA. Cumulative ERP change (ERP difference between P + VS and P + atropine) was greatest in the LAA and corresponded with expression of Kir3.1/3.4 (LAA > PLA ≥ PV). The ERP change in response to vagal manipulation was most heterogeneous in the PLA; this corresponded with a pronounced heterogeneity of Kir3.1 distribution in the PLA. With VS and/or P, there was evidence of regional conduction delay in the PVs with a significant change in activation direction. Similar activation changes were not seen in the PLA and LAA.

Conclusions The PVs and PLA demonstrate unique activation and repolarization characteristics in response to autonomic manipulation. The heterogeneity of vagal responses correlates with the pattern of IKAch distribution in the LA. The peculiar autonomic characteristics of the PVs and PLA might create substrate for re-entry and AF. (J Am Coll Cardiol 2007;49:1340–8) © 2007 by the American College of Cardiology Foundation

The pulmonary veins (PVs) have recently been shown to play a major role in the genesis of atrial fibrillation (AF) (1).

See page 1349

The PVs and the adjoining left atrium (LA) have been shown to have unique electrophysiologic characteristics as compared with the rest of the LA, at least partially owing to underlying structural heterogeneities (2). Focal "triggers" and "drivers" in the PV also seem to be significantly modified or regulated by the autonomic nervous system (3).

Atrial fibrillation has been shown to occur in the setting of a heightened sympathetic state (i.e., "adrenergic" AF) as well as in the presence of increased vagal tone (i.e., "vagal" AF) (4,5). A greater role for the parasympathetic nervous system in focal AF has been recently postulated (6). More recent studies suggest that complex interactions between the 2 limbs of the autonomic nervous system might be involved in the genesis of AF (7). Nonetheless, the detailed autonomic profile of the PVs—especially as it compares with the posterior left atrium (PLA) and the rest of the LA—has not been well characterized.

We hypothesized that the LA exhibits a heterogeneous electrophysiologic response to autonomic maneuvers, with the activation and repolarization characteristics of the PVs being different from the rest of the LA. Because IKAch is the ion channel that is primarily responsible for vagal effects on LA refractoriness, we further hypothesized that interregional variation in repolarization (in response to vagal maneuvers) is due to differences in the expression and spatial distribution of IKAch within the PVs, PLA, and left atrial appendage (LAA).

From the Division of Cardiology and Department of Medicine, Northwestern University-Feinberg School of Medicine, Chicago, Illinois. This work was supported by the National Institutes of Health (National Heart, Lung, and Blood Institute) grant 5K08HL074192; Northwestern University–Feinberg School of Medicine; the Everett O'Connor Trust; and Medtronic, Inc.

Manuscript received May 9, 2006; revised manuscript received October 23, 2006, accepted October 29, 2006.

Methods

The investigation conforms to the Guide for the Care and Use of Laboratory Animals published by the U.S. National Institutes of Health (NIH Publication No. 85-23, revised 1996). Approval for use of purpose-bred dogs (hounds) was obtained from the institutional animal use committee.

Mapping protocol. All procedures were performed in normal dogs under general anesthesia (2.5% isoflurane). The left cervical vagus was isolated in the neck; the vagus at this level consists entirely of parasympathetic fibers (8). The chest was then opened via a left-sided thoracotomy. High-density plaques were sutured onto the left inferior PV (8 × 5 electrodes; 2.5-mm interelectrode spacing), the PLA (7 × 3 electrodes; 5-mm interelectrode spacing), and LAA (7 × 3 electrodes; 5-mm interelectrode spacing) for bipolar electrogram recording and pacing. The PV plaque was placed circumferentially around the vein, so as to encircle two-thirds of the venous circumference. The other 2 plaques were laid flat on the surface of the PLA and LAA, respectively.

All data were acquired by a 128-channel mapping system (Prucka Cardiolab, GE, Milwaukee, Wisconsin) at a sampling rate of 977 Hz. Mapping of activation patterns was performed at each location in sinus rhythm as well as during LA pacing at 400 ms under the following conditions: 1) baseline; 2) left cervical vagal stimulation (VS); 3) beta-blockade (propranolol 0.2 mg/kg, then 0.04 mg/kg/h) (P); 4) beta-blockade + vagal stimulation (P + VS); and 5) propranolol + atropine (0.04 mg/kg, then 0.007 mg/kg/h) (P + ATR). The left vagus was stimulated, because it is primarily responsible for the innervation of the left sided PVs, PLA, and LAA (8). The VS was performed at 20 Hz (15V to 20V, 2 ms to 8 ms) (Grass S44G, Astromed, West Warwick, Rhode Island); a response consisted of: 1) sinus node slowing by at least 25%, or 2) PR prolongation by more than 25% or 2:1 atrioventricular block. Only animals in which a vagal response was obtained were used for analysis.

During each of the aforementioned maneuvers, effective refractory periods (ERPs) were measured at 10 ± 3 sites in the PV, 6 ± 2 sites in the PLA, and 5 ± 3 sites in the LAA. A drive train of 8 stimuli was given (S1 = 400 ms) at twice diastolic threshold, followed by a single extrastimulus (S2); S2 was decremented by 10 ms until local ERP was reached. Each set of ERP measurements (in response to a particular intervention) took approximately 15 min to perform. Because vagal effects were seen almost instantaneously after the initiation of VS, an equilibrium time of <1 min was used with VS. With propranolol or atropine administration, an equilibration time of 30 min was used.

In 5 animals, ERPs were measured at more than 1 time interval (30 min to 2 h apart) to assess for consistency in ERP response. Both baseline ERPs as well as ERPs in response to VS were found to be constant (± 10 ms) at each site over 2 or more intervals.

Atrial fibrillation was induced several times with ERP testing during VS from the PV, PLA, as well as the LAA. In almost all instances, AF terminated within 5 s after cessation of VS. The ERP testing was therefore resumed within 1 min of AF termination. At the end of the mapping protocol, animals were killed, and the hearts were removed for western blotting and immunohistochemistry.

Abbreviations and Acronyms

AF = atrial fibrillation
ATR = atropine
ERP = effective refractory period
LA = left atrium
LAA = left atrial appendage
P = propranolol
PLA = posterior left atrium
PV = pulmonary vein
VS = vagal stimulation

Western blotting. Proteins were extracted from frozen PV, PLA, and LAA biopsies (from 8 animals), solubilized in Laemmli sample buffer and subjected to sodium dodecyl sulfate polyacrylamide gel electrophoresis (SDS-PAGE) with 10% acrylamide gels (Bio-Rad, Hercules, California). Electrophoresed proteins were then transferred to nitrocellulose membranes for immunoblot analysis. Nonspecific protein-binding sites were blocked with phosphate-buffered saline containing 5% milk. Membranes were incubated with polyclonal antibodies against Kir3.1 and Kir3.4 (Alomone Labs, Jerusalem, Israel) in dilutions of 1:500 or 1:1000. Peroxidase-conjugated secondary antibodies, diluted 1:5000 or 1:10000 (Pierce, Rockford, Illinois), were used to detect bound primary antibody. Protein bands were visualized via enhanced chemiluminescence (Amersham, Arlington Heights, Illinois). All bands were quantified with standard software (Image J, National Institutes of Health, Bethesda, Maryland). The signal for both proteins was normalized to total alpha-actin expression. Of these 8 animals, 3 also underwent electrophysiologic testing.

Immunohistochemistry. Frozen samples of PV, PLA, and LAA from 5 dogs were sectioned at 5 microns, allowed to air-dry overnight, and fixed in an acetone/alcohol mixture. Endogenous peroxidase was blocked with dual endogenous enzyme block (DAKO, Carpinteria, California), and nonspecific staining was blocked with a serum-free protein block (DAKO). Sections were incubated for 1 h with anti-Kir3.1 antibody (Alomone Labs) followed by an anti-rabbit dextran polymer conjugated to horseradish peroxidase (HRP) (DAKO) for 30 min and visualized with diaminobenzidine (DAKO). Sections were counterstained with Mayer's hematoxylin (Sigma, St. Louis, Missouri), dehydrated to xylene, and mounted with cover glass. All 5 of these animals also underwent electrophysiologic testing.

Data analysis. For each location and condition, the average ERP for all sites at that location was determined. The ERP changes in response to the aforementioned maneuvers were compared between the different conditions and regions. The ERP difference between P + VS (i.e., full vagal effect with no sympathetic effect) and P + ATR (no vagal and no sympathetic effect) was determined for each region as a

JACC Vol. 49, No. 12, 2007
March 27, 2007:1340–8

measure of the entire range of vagal effect on refractoriness (i.e., "cumulative" vagal effect). The variance of the cumulative vagal effect was obtained as a measure of the heterogeneity of vagal response within each region.

Post-acquisition analysis of activation direction was performed with the use of MATLAB (Mathworks, Natick, Massachusetts). The first rapid deflection of each atrial electrogram was marked to time local activation. Activation (isochronal) maps were constructed for each region and each intervention during sinus rhythm as well as during LA pacing. The PV activation maps were compared in 3 dogs at a resolution of 2.5 mm as well as for 5-mm spacing (at the same site). Activation direction within the PV was found to be similar for both inter-electrode distances.

In addition, conduction velocity vectors (m/s) were calculated at each electrode with the gradient of the activation times and compared among regions and interventions. To better quantify changes in activation direction with each intervention, conduction velocities in the X- and Y-direction at each location were also determined (9). The X- and Y-directions for each region were as follows: PV: X = along the PV circumference (i.e., perpendicular to the PV long axis), Y = proximal-to-distal PV (i.e., PV long axis); PLA: X = along the atrioventricular groove, Y = from atrioventricular groove to base of superior PVs; LAA: X = parallel to base of LAA, Y = from base-to-apex of LAA.

Immunohistochemical data were analyzed for heterogeneity of Kir3.1 expression in the PV, PLA, and LAA. For this purpose, Kir3.1 staining was performed in 3 dogs. In each region of each animal, the number of myocardial cells that stained for Kir3.1 were individually counted in 6, randomly selected 40× fields. The variance of these counts was obtained for each region, as a measure of heterogeneity of expression of Kir3.1 (and IKAch).

Statistical analysis. Continuous data are presented as mean ± SEM. A hierarchical mixed-effects model was used to analyze the data, with the effects of dogs and electrodes (nested within dogs) treated as random factors. The HLM version 6 software from Scientific Software International (Lincolnwood, Illinois) was used to carry out the analyses. A restricted maximum-likelihood estimation approach was applied, and information from all available data-points was used. Unconditional variance-covariance structure was used where no variance or covariance parameters were assumed to be equal. Comparisons of ERP values among regions were made independently for each of the experimental stages. In addition, the ERP difference between P + ATR and P + VS ("cumulative vagal effect") was also estimated independently of the data collected during remaining stages.

Heterogeneity of Kir3.1 expression in immunostained specimens was quantified by the variance (SD^2). Variances between regions were compared with the Levene's test, treating intra-dog variation as a random variable. Statistical significance was evaluated at a 5%, 2-tailed level.

Results

Fourteen normal, healthy dogs underwent electrophysiologic testing. At baseline, ERP was longest in the PV and shortest in the LAA (LAA < PV, p = 0.001; LAA < PLA, p = 0.07; PLA < PV, p = 0.06) (Fig. 1A). Conduction velocity at baseline was slower in the PV and PLA as compared with the LAA (LAA > PV, p = 0.01; LAA > PLA, p = 0.047; PLA approximately = PV, p = 0.65) (Table 1). These values are consistent with those previously published in the literature (10).

On average, pacing thresholds (mA) were higher in the PVs than in the rest of the atrium (PV = 2.5 ± 1.9, PLA = 1.9 ± 1.3, LAA = 1.0 ± 1.4, p < 0.01). Pacing thresholds were more homogenous in the LAA than in the PLA and PV (p < 0.05 for variance comparison between regions).

ERP changes in response to autonomic maneuvers. In response to VS, there was a significant decrease in ERP (9%) in the PV as compared with baseline (p = 0.001) (Fig. 1A). In contrast, ERP changes in the PLA and LAA in response to VS were not as pronounced.

In the presence of beta-blockade, vagal stimulation (P + VS) resulted in a more pronounced decrease in ERP

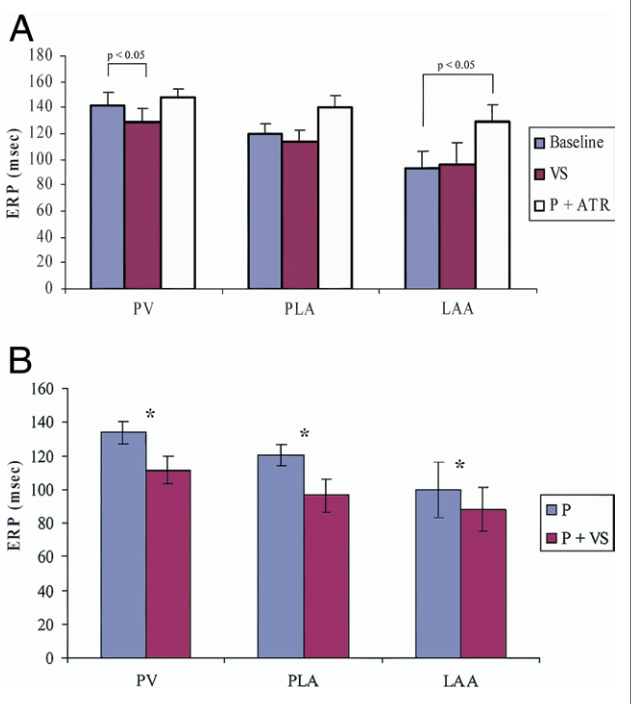

Figure 1 Variations in Regional ERP Response With Miscellaneous Autonomic Maneuvers

(A) Comparison of vagal stimulation (VS) versus baseline indicates parasympathetic responsiveness in the resting state; this was most pronounced in the pulmonary vein (PV). Comparison of propranolol (P) + atropine (ATR) versus baseline indicates resting vagal tone, which was greatest in the left atrial appendage (LAA). **(B)** With P + VS, more pronounced effective refractory period (ERP) shortening was noted in the PV, posterior left atrium (PLA), and LAA as compared with ERP shortening with VS alone. See text for discussion. *p < 0.05.

Table 1 Conduction Velocity (m/s) in Response to Autonomic Maneuvers

	Baseline	VS	P	P + VS	P + ATR
PV	1.4 ± 0.1	1.3 ± 0.1	1.5 ± 0.1	1.4 ± 0.1	1.2 ± 0.1
PLA	1.5 ± 0.1	1.5 ± 0.1	1.7 ± 0.1	1.5 ± 0.1	1.7 ± 0.1
LAA	2.1 ± 0.1	2.0 ± 0.1	2.0 ± 0.1	1.8 ± 0.1	1.9 ± 0.2

Baseline differences between the regions are discussed in the text.
ATR = atropine; LAA = left atrial appendage; P = propranolol; PLA = posterior left atrium; PV = pulmonary vein; VS = vagal stimulation.

in the PV (17.7%), PLA (19.9%), and LAA (11.6%) (P + VS vs. P − PV: $p < 0.001$, PLA: $p = 0.003$, LAA: $p = 0.036$) (Fig. 1B) as compared with VS alone. The ERP decrease in the PV and PLA was significantly greater than in the LAA ($p < 0.05$).

As compared with baseline, double autonomic blockade (P + ATR) caused a marked increase (38.2%) in ERP in the LAA (P + ATR vs. baseline: $p = 0.004$) (Fig. 1A) and a less pronounced increase (17.3%) in the PLA (P + ATR vs. baseline: $p = 0.135$). In contrast, there was no significant change in ERP in the PV in response to P + ATR.

The ERP heterogeneity (as measured by variance) in each region was greater in the presence of maximal vagal stimulation (P + VS) than in the presence of vagal blockade (P + ATR) (P + VS > P + ATR, $p < 0.01$).

Regional differences in vagal effect—correlation with IKAch distribution. Cumulative vagal effect (ERP difference between P + VS and P + ATR) was found to be greatest in the LAA (ERP change: LAA > PV, $p = 0.04$; LAA ≥ PLA, $p = 0.12$) (Fig. 2A). Eight dogs had western blotting performed for Kir3.1/3.4; 3 of these dogs also underwent electrophysiologic testing. The cumulative vagal effect in the PV, PLA, and LAA corresponded to the relative expression of the IKAch subunits Kir3.1 and Kir3.4 in these regions (for both Kir3.1 and 3.4, LAA > PLA ≥ PV) (Figs. 2B and 2C); differences in regional Kir3.1 and 3.4 expression were consistent across all animals. However, vagal-induced ERP shortening was significantly more heterogenous in the PLA as compared with the LAA (variance of ERP shortening: PLA > LAA, $p = 0.04$) (Fig. 3). Heterogeneity of ERP shortening (in all dogs as well as in the 5 dogs that underwent immunohistochemical staining) corresponded to the heterogeneity of IKAch distribution in each region (variance of the number of Kir3.1 positive cells counted under 6 high-power (40×) fields: PV approximately = PLA > LAA, $p < 0.01$). Figures 3B and 3C show a typical example of greater heterogeneity of Kir3.1 expression in the PLA as compared with the LAA. Heterogeneity of Kir3.1 was consistent within multiple samples from a particular region.

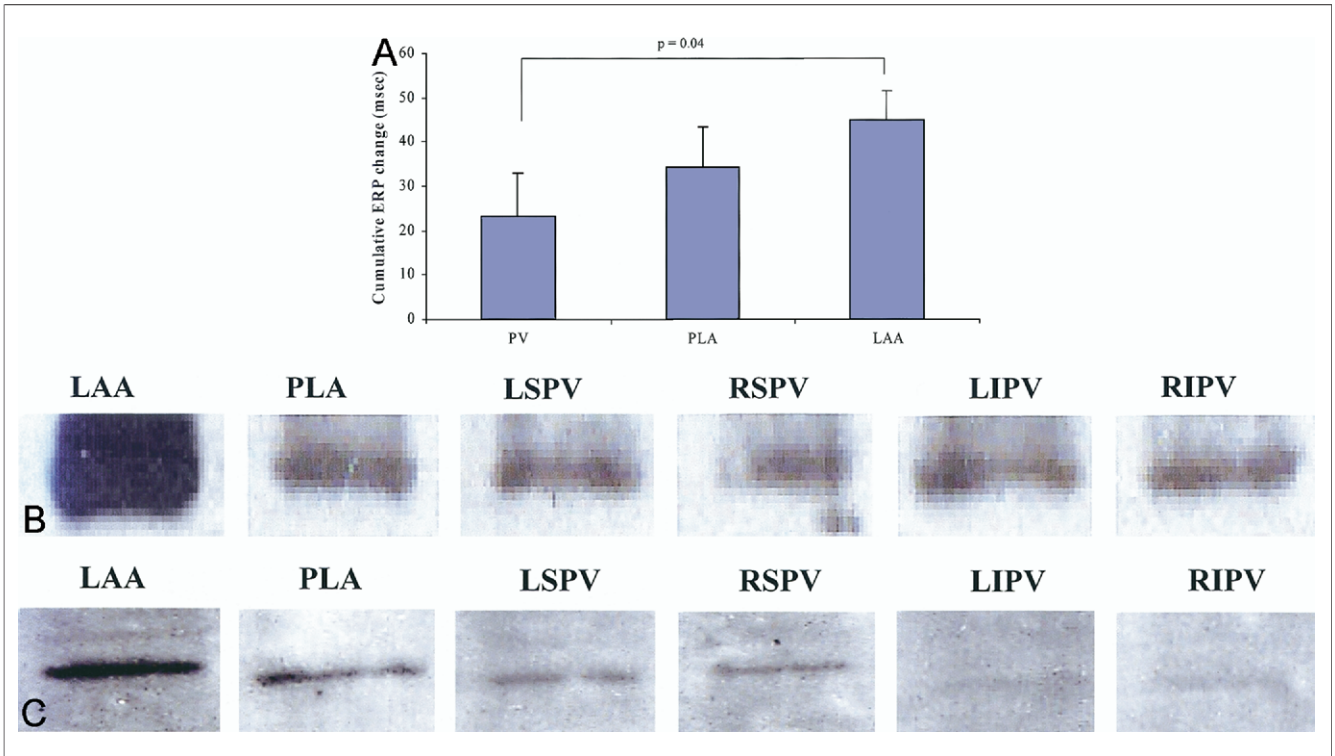

Figure 2 Heterogeneity of Cumulative Vagal Effect in the Left Atrium and Its Correlation With IKAch (Kir3.1/3.4) Expression in the PV, PLA, and LAA

(A) The panel shows cumulative vagal effect as measured by the ERP difference between P + VS and P + ATR. The cumulative vagal effect is greatest in the LAA, followed by the PLA and PV (LAA > PLA ≥ PV). Panels **B** and **C** show western blots for Kir3.1 and 3.4, respectively. Each protein shows greatest expression in the LAA, followed by the PLA and PV (LAA > PLA ≥ PV). LSPV = left superior pulmonary vein; LIPV = left inferior pulmonary vein; RIPV = right inferior pulmonary vein; RSPV = right superior pulmonary vein; other abbreviations as in Figure 1.

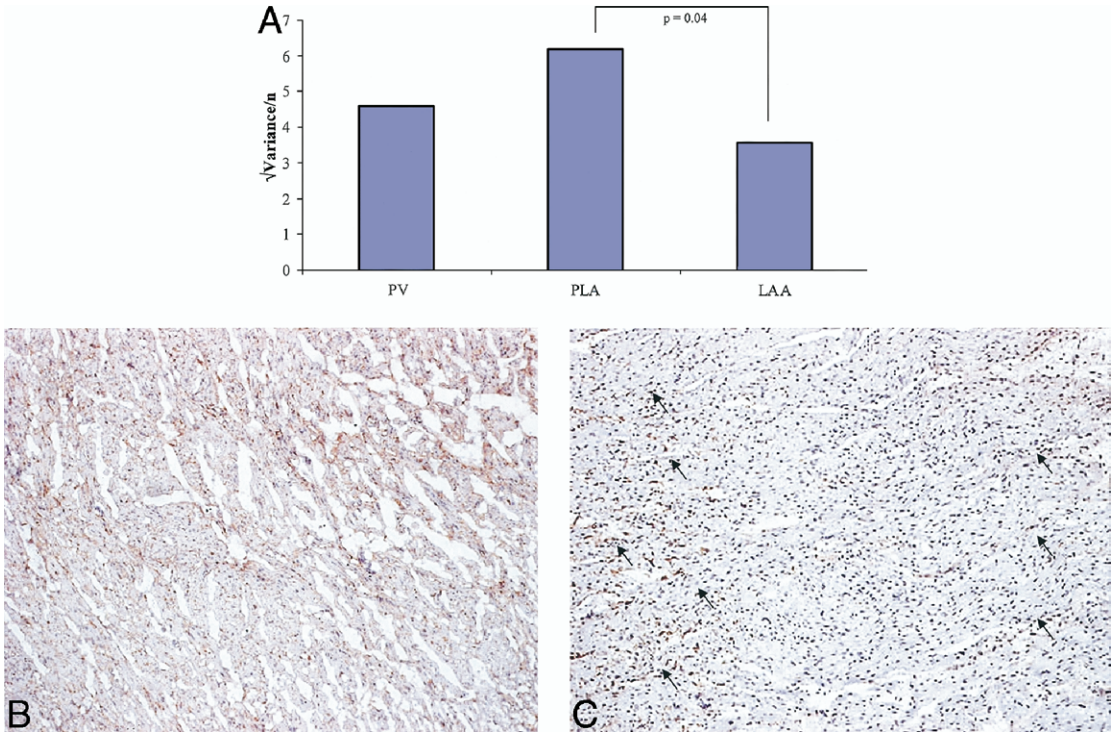

Figure 3 **Heterogeneity of Vagal-Induced ERP Shortening Within the PV, PLA, and LAA Corresponds With Heterogeneity of IKAch Distribution Within Each Region**

(A) The panel shows heterogeneity of ERP shortening among individual pacing electrodes in the PV, PLA, and LAA. Interelectrode heterogeneity (√Variance/N) is the greatest in the PLA and is least in the LAA. **Panels B and C** show examples of immunostaining (10× magnification) for Kir3.1 in the LAA and PLA, respectively. The Kir3.1 is **stained red**. In the LAA **(B)**, Kir3.1 staining is very homogeneous. In contrast, staining for Kir3.1 is significantly more heterogeneous in the PLA **(C)**. The **black arrows** indicate the heterogeneity of red staining in the PLA. Abbreviations as in Figure 1.

Activation and conduction patterns. All activation and conduction patterns were analyzed during sinus rhythm. Sinus cycle length was >400 ms at baseline as well as with each autonomic intervention (data not shown). Because these rates were significantly greater than the ERPs noted with each intervention and in each region (Fig. 1), the activation changes observed in response to different autonomic maneuvers cannot be attributed to regional changes in refractory periods. Despite changes in sinus rate, there was no significant change in surface P-wave morphology (as assessed in multiple leads by 2 independent observers) with any autonomic intervention; this confirmed that the rhythm was sinus (and not an ectopic atrial rhythm) during each intervention.

Total conduction velocity did not change significantly from baseline in the PV, PLA, or LAA in response to autonomic maneuvers (Table 1). However, the direction of activation during sinus rhythm—and resulting activation patterns—were noted to change markedly in the PV in response to VS as well as in response to beta-blockade. In contrast to the PV, activation direction did not change significantly in the PLA and LAA in response to autonomic maneuvers.

Figures 4A and 4B demonstrate an example of a marked change in the site of earliest activation ("breakout") in the PV in the presence of beta-blockade (as compared with baseline), with breakout occurring at the opposite sides of the mapped region in the presence and absence of beta-blockade. Figures 4C to 4F show activation maps in the PLA and LAA in the same dog, at baseline and in the presence of beta-blockade. Unlike in the PV, activation patterns remained relatively unchanged in the PLA and LAA. Activation patterns were also assessed during LA pacing at 400 ms. As with sinus rhythm, activation changes were most pronounced in the PV; Figure 5 shows a significant change in the site of earliest activation in the PV in the presence of beta-blockade.

Activation along X- and Y-axis. Analysis of the directional (X/Y) components of the baseline conduction velocity revealed a difference between activation along the X- versus the Y-axis in the PLA and LAA (PLA: X vs. Y, $p = 0.175$; LAA: X vs. Y, $p = 0.017$) (Fig. 6). X- and Y-components were approximately equal in the PVs at baseline (X vs. Y, p = NS).

Assessment of the X- and Y-components of conduction velocity in each region confirmed the changes in activation direction noted in the PV in response to VS and beta-

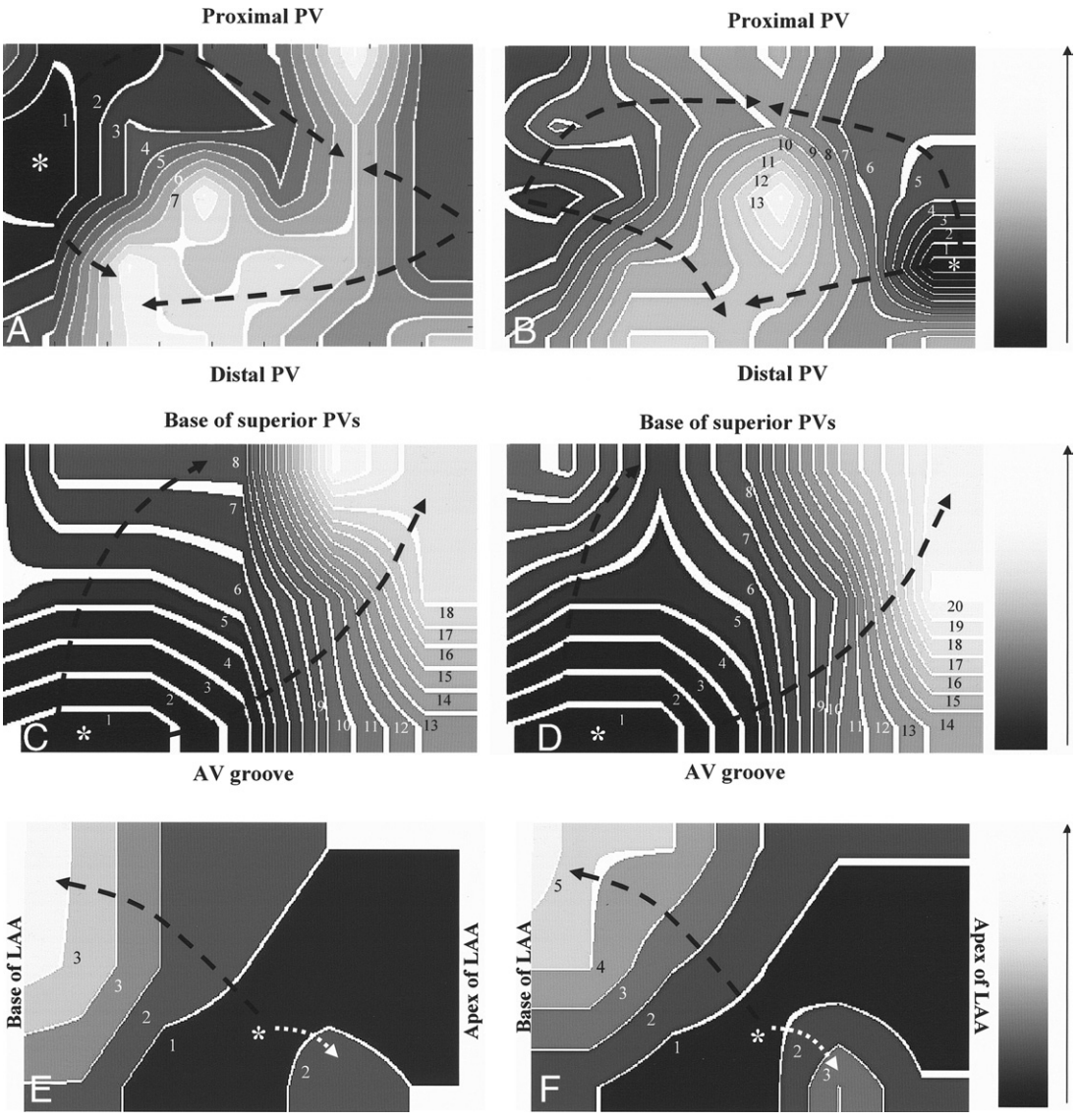

Figure 4 **Activation Change in the PV With P**

Panels A, C, and E represent baseline activation during sinus rhythm in the PV, PLA, and LAA, respectively. **Panels B, D, and F** represent activation in the PV, PLA, and LAA in the presence of P. **(A)** At baseline, earliest activation is noted on the left side of the plaque **(*)**. **(B)** With P, earliest activation shifts to the opposite end of the plaque **(*)**. No significant differences are noted in earliest activation or activation direction in the PLA **(C, E)** or in the LAA **(E, F)** in the presence of P. Each isochronal step represents 1 ms. *Earliest activation. The grid on the **right** shows that earliest activation is **black**, with later times indicated by progressively decreasing **shades of gray**. Abbreviations as in Figure 1.

blockade. As compared with baseline, the PVs demonstrated a decrease in the magnitude of the Y-vector in response to VS ($Y_{VS} < Y_{base} = 0.06 \pm 0.06 < 0.18 \pm 0.07$, $p = 0.046$) (Fig. 6A) as well as a significant change in X/Y ratio in response to P and to P + VS (X_{base} vs. Y_{base} = 0.10 ± 0.06 vs. 0.18 ± 0.07, p = NS; X_P vs. $Y_P = 0.21 \pm 0.08$ vs. 0.02 ± 0.09, $p = 0.02$; $X_{P + VS}$ vs. $Y_{P + VS}$ = 0.24 ± 0.10 vs. 0.06 ± 0.06; $p = 0.04$) (Fig. 6A), indicating a significant change in activation direction in response to these maneuvers. In contrast, the X/Y relationship remained relatively unaltered in the PLA and LAA in response to these autonomic maneuvers, indicating no significant change in activation in these regions (Figs. 6B and 6C).

Discussion

The major finding of this study is that the LA and PVs demonstrate a heterogeneous response to autonomic maneuvers. The overall vagal contribution to refractoriness is greater in the LAA than in the PVs and PLA, largely owing to a higher resting vagal tone in the LAA. Even though the resting vagal tone is higher in the LAA, VS causes a greater

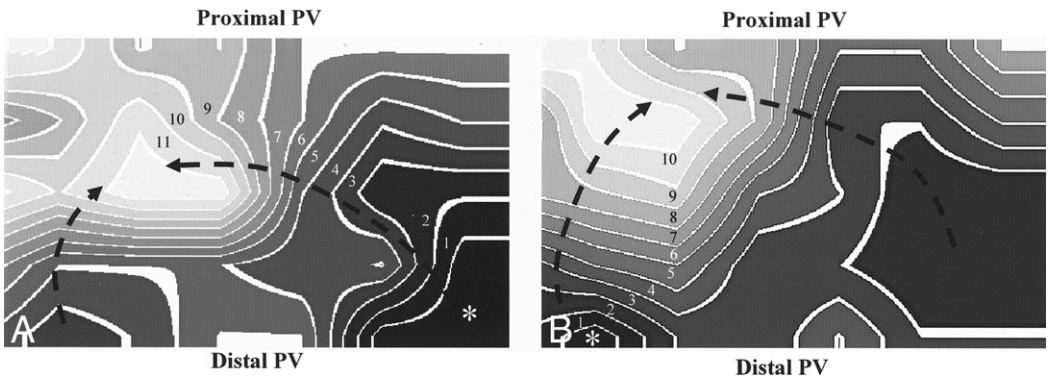

Figure 5 **Activation Change in the PV With P**

Panels A and B represent 1 PV in the presence and absence of P, during pacing at 400 ms. **(A)** At baseline, earliest activation **(*)** is noted at the **lower right** (distal PV), indicating breakout in the unmapped posterior one-third of the PV. **(B)** With P, earliest activation **(*)** shifts to the opposite end **(left)** of the distal PV, with a resulting change in the direction of activation. Each isochronal step represents 1 ms. Abbreviations as in Figure 1.

decrease in ERP in the PV and PLA (as compared with the LAA). Moreover, the heterogeneity of vagal effects on refractoriness is more pronounced in the PLA as compared with the PV and LAA. The effects of VS on refractoriness are consistent with the relative pattern of distribution of IKAch in these regions.

In addition to heterogeneous repolarization effects seen in response to autonomic maneuvers, the PVs demonstrated unique activation characteristics in the presence of VS and/or beta-blockade. With either of these maneuvers, the PVs demonstrated regional conduction block and significant change in the direction of activation as compared with baseline. In contrast, similar activation changes were not noted in the PLA or LAA.

Unique repolarization profile of the PVs and PLA: role of IKAch. Recent clinical studies have shown that in some cases AF can be caused by a rapidly firing focus in the PVs (1). Clinical and animal data suggest that these PV triggers and drivers seem to be at least partially modulated by the autonomic nervous system (3). More recently, Pappone et al. (6) have suggested that altering vagal input to the PLA and the PVs—as measured by the elimination of vagal reflexes on PV stimulation—might improve efficacy of ablation procedures for AF.

Despite these initial studies, the detailed autonomic profile of the PVs and the PLA and the precise role of the autonomic nervous system in the genesis of focal AF have not been systematically investigated in animal or clinical models. In this electrophysiologic study, we demonstrate unique differences in autonomic responsiveness among the PVs, PLA, and the rest of the LA. The heterogeneity of autonomic responsiveness in the LA is at least partially explained by the differential distribution of IKAch that we have demonstrated in the LA. The IKAch is the predominant ion-channel responsible for vagal effects on refractoriness in the LA (11), with muscarinic receptors activating IKAch via G-protein–dependent pathways. As a result, IKAch is believed to play a key role in vagal influences on AF substrate (12). The IKAch concentrations have been shown to be greater in the LA than in the RA (13). However, the heterogeneity of IKAch expression within the LA has not been previously described. In this study, we demonstrate differences in the expression of IKAch within different regions of the LA and PVs, with total IKAch expression being greater in the LAA than in the PVs or PLA. In addition to differences in overall expression of IKAch among the PV, PLA, and LAA, we have also demonstrated differences in spatial distribution of IKAch within each of these regions. Distribution of IKAch seems to be most heterogenous within the PLA; this is consistent with the heterogeneous ERP response to VS that was noted in the PLA.

Unique activation profile of the PVs. The PV activation changes that we have demonstrated in the current study suggest that vagal and/or adrenergic manipulation might also contribute to creation of functional conduction block in the PVs. In fact, both vagal and sympathetic manipulation have been shown to influence gap-junction conduction and set up substrate for re-entry in relatively uncoupled myocardial tissue (14–16). The heterogeneity of fiber orientation and the relatively uncoupled state that exist in the PVs as compared with the LA (2,17) might therefore make them particularly sensitive to parasympathetically and sympathetically modulated changes in conduction.

Implications for re-entry. With high-resolution optical mapping, Arora et al. (10) demonstrated substrate for re-entry at the PV-LA junction; in this ex vivo study, re-entry could be sustained in Landendorff-perfused PVs only in the presence of isoproterenol or acetylcholine. Therefore, both sympathetic and parasympathetic manipulation seem capable of creating conditions for re-entry in the PVs—albeit by potentially different mechanisms. Because acetylcholine has previously been shown

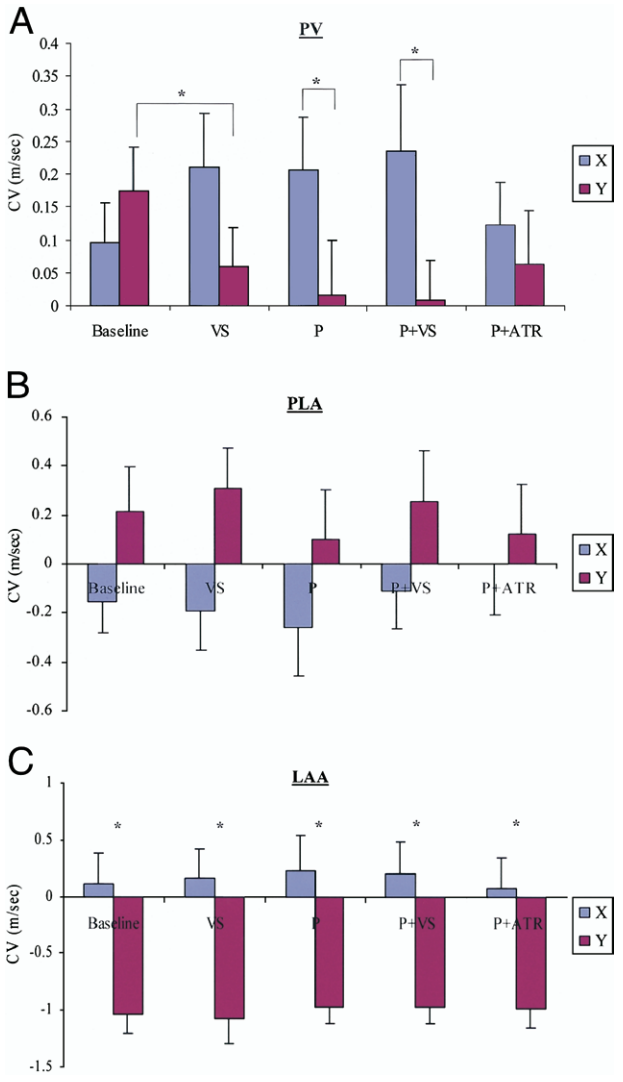

Figure 6 **X- and Y-Conduction Vectors in Response to Autonomic Maneuvers**

Each **panel** shows X- and Y-components of conduction velocity for each region and for each intervention. **(A)** In the PV, VS, P, and P + VS cause a significant change in the Y-vector and the resulting X/Y relationship, indicating a change in activation direction. **Panels B and C** show X- and Y-vectors for the PLA and LAA, respectively. In both regions, there was no significant change in either X- or Y-component or in the X/Y relationship in response to any intervention. *p ≤ 0.05 (X vs. Y). Abbreviations as in Figure 1.

to cause sustained re-entry at the PV-LA junction in Langendorff preparations (10), it is conceivable—on the basis of the results of the current study—that VS might be creating substrate for functional re-entry by shortening refractoriness preferentially and heterogeneously within the PLA.

Sympatho-vagal interactions. Recent physiology studies by Patterson et al. (7) suggest that adrenergic influences might be playing an important modulatory role in the emergence of focal triggers/drivers in the presence of an increased vagal tone.

Significant sympatho-vagal interactions were also noted in the current study. Beta-blockade accentuated vagal-induced ERP shortening in each region, thereby suggesting that sympathetic stimulation might be antagonistic to vagal effects in the LA. Of note, ERP shortening caused by P + VS was more pronounced in the PLA and LAA (as compared with the PV), indicating a heterogeneity of sympatho-vagal interactions within the LA.

Study limitations. This was a canine study, the results of which cannot be directly extrapolated to the human LA. Moreover, this study was conducted in normal dogs, and it is not known to what extent autonomic remodeling contributes to AF substrate in the setting of structural heart disease.

The distribution of autonomic nerves in the LA and PVs was not examined in this study; heterogeneity of nerve distribution and differences in sympathetic/parasympathetic co-localization (18) within the LA might play a role in the creation of substrate for focal AF. Although AF was more readily inducible in the presence of VS, AF inducibility and characteristics of the induced AF were not examined in detail in this study.

Although vagal responses have been shown to be more pronounced in the left superior PV, electrophysiologic testing was performed only on the left inferior PV (because it was the easiest vein to access via a left-sided thoracotomy). Nonetheless, the left inferior PV was felt to be a suitable vein for this study, because significant vagal responses have been described during ablation in and around this vein (6).

Immunostaining (for Kir3.1 heterogeneity) was performed only on sections from the epicardial aspect of the PV, PLA, and LAA (because these were the surfaces that were mapped); heterogeneity of Kir3.1 distribution was not separately assessed for the endocardium.

Conclusions

This study demonstrates the presence of a unique autonomic profile in the PVs and PLA; the repolarization profile seems to correlate with the underlying pattern of distribution of IKAch. The peculiar autonomic characteristics of this region might contribute to the genesis of focal AF.

Acknowledgment

The authors thank Pablo Denes, MD, for critical review of the manuscript.

Reprint requests and correspondence: Dr. Alan H. Kadish, Northwestern Memorial Hospital, 251 East Huron, Feinberg 8-542, Chicago, Illinois 60611. E-mail: a-kadish@northwestern.edu.

REFERENCES

1. Haissaguerre M, Jais P, Shah DC, et al. Spontaneous initiation of atrial fibrillation by ectopic beats originating in the pulmonary veins. N Engl J Med 1998;339:659–66.

2. Hocini M, Ho SY, Kawara T, et al. Electrical conduction in canine pulmonary veins: electrophysiological and anatomic correlation. Circulation 2002;105:2442–8.
3. Schauerte P, Scherlag B, Patterson E, et al. Focal atrial fibrillation: experimental evidence for a pathophysiologic role of the autonomic nervous system. J Cardiovasc Electrophysiol 2001;12:592–9.
4. Amar D, Zhang H, Miodownik S, Kadish AH. Competing autonomic mechanisms precede the onset of postoperative atrial fibrillation. J Am Coll Cardiol 2003;42:1262–8.
5. Oral H, Chugh A, Scharf C, et al. Pulmonary vein isolation for vagotonic, adrenergic, and random episodes of paroxysmal atrial fibrillation. J Cardiovasc Electrophysiol 2004;15:402–6.
6. Pappone C, Santinelli V, Manguso F, et al. Pulmonary vein denervation enhances long-term benefit after circumferential ablation for paroxysmal atrial fibrillation. Circulation 2004;109:327–34.
7. Patterson E, Po S, Scherlag BJ, Lazzara R. Triggered firing in pulmonary veins initiated by in vitro autonomic nerve stimulation. Heart Rhythm 2005;2:624–31.
8. Ulphani J, Cain J, Inderyas F, et al. Parasympathetic innervations of the posterior left atrium primarily originate in the Ligament of Marshall. Circulation 2005;112:II–189.
9. Nanthakumar K, Huang J, Rogers JM, et al. Regional differences in ventricular fibrillation in the open-chest porcine left ventricle. Circ Res 2002;91:733–40.
10. Arora R, Verheule S, Scott L, et al. Arrhythmogenic substrate of the pulmonary veins assessed by high-resolution optical mapping. Circulation 2003;107:1816–21.
11. Lomax AE, Rose RA, Giles WR. Electrophysiological evidence for a gradient of G protein-gated K+ current in adult mouse atria. Br J Pharmacol 2003;140:576–84.
12. Dobrev D, Friedrich A, Voigt N, et al. The G protein-gated potassium current I (K,ACh) is constitutively active in patients with chronic atrial fibrillation. Circulation 2005;112:3697–706.
13. Sarmast F, Kolli A, Zaitsev A, et al. Cholinergic atrial fibrillation: I (K,ACh) gradients determine unequal left/right atrial frequencies and rotor dynamics. Cardiovasc Res 2003;59:863–73.
14. Ando M, Katare R, Kakinuma Y, et al. Efferent vagal nerve stimulation protects heart against ischemia-induced arrhythmias by preserving connexin43 protein. Circulation 2005;112:164–70.
15. Slovut DP, Mehta S, Dorrance AM, Brosius FC, Watts SW, Webb RC. Increased vascular sensitivity and connexin43 expression after sympathetic denervation. Cardiovasc Res 2004;62:388–96.
16. Arutunyan A, Pumir A, Krinsky V, Swift L, Sarvazyan N. Behavior of ectopic surface: effects of beta-adrenergic stimulation and uncoupling. Am J Physiol Heart Circ Physiol 2003;285:H2531–42.
17. Verheule S, Wilson E, Arora R, Engle SK, Scott LR, Olgin JE. Tissue structure and connexin expression of canine pulmonary veins. Cardiovasc Res 2002;55:727–38.
18. Tan AY, Li H, Wachsmann-Hogiu S, Chen LS, Chen PS, Fishbein MC. Autonomic innervation and segmental muscular disconnections at the human pulmonary vein-atrial junction: implications for catheter ablation of atrial-pulmonary vein junction. J Am Coll Cardiol 2006;48:132–43.